Author(s): Shim, Jihye & Lee, Eok-Kyun & Lee, Young Joo & Nieminen, Risto M.

Title: Density-functional calculations of defect formation energies using the supercell method: Brillouin-zone sampling

Year: 2005

Version: Final published version

Please cite the original version:

Shim, Jihye & Lee, Eok-Kyun & Lee, Young Joo & Nieminen, Risto M. 2005. Density-functional calculations of defect formation energies using the supercell method: Brillouin-zone sampling. Physical Review B. Volume 71, Issue 24. 245204/1-7. ISSN 1550-235X (electronic). DOI: 10.1103/physrevb.71.245204.

Density-functional calculations of defect formation energies using the supercell method: Brillouin-zone sampling

Jihye Shim and Eok-Kyun Lee
Department of Chemistry and School of Molecular Science (BK21), Korea Advanced Institute of Science and Technology, Taejon, Korea

Young Joo Lee
New Materials and Components Research Center, Research Institute of Industrial Science and Technology, P.O.Box 135, Pohang, 790-330, Korea

Risto M. Nieminen
Laboratory of Physics, Helsinki University of Technology, P.O. Box 1100, FIN-02015 HUT, Finland
(Received 19 January 2005; published 27 June 2005)

Using the DFT supercell method, the BZ sampling error in the formation energy and atomic structure are investigated for vacancy and interstitial defects in diamond and silicon. We find that the **k**-point sampling errors in the total energy vary considerably depending on the charge state and defect type without systematic cancellation, even for the same size of supercell. The error in the total energy increases with decreasing electronic perturbation of the defect system relative to the perfect bulk; this effect originates in the localization of electronic states due to the symmetry reduction induced by the presence of a defect. The error in the total energy is directly transferred to the formation energy, and consequently changes the thermodynamic stability of charge states and shifts the ionization levels. In addition, in force calculations and atomic structure determinations, the **k**-point sampling error is observed to increase as the charge becomes more negative. The Γ-point sampling results in erroneously large relaxation of the four atoms surrounding a vacancy in diamond. We suggest that stronger repulsions between electrons occupying degenerate defect levels at Γ-point compared to those occupying split energy levels at other **k** points induces larger atomic movements.

DOI: 10.1103/PhysRevB.71.245204 PACS number(s): 71.55.Cn, 71.15.Dx, 71.20.Mq

I. INTRODUCTION

In supercell calculations, the total energy of the system is calculated by sampling the Brillouin zone (BZ). However, the computational load grows linearly with the number of **k** points, and two wave functions with similar wavevectors on a given band are expected to be very similar.[1] Thus, in order to minimize the computational effort, the eigenvalues and eigenfunctions are calculated on special sets comprised of a finite number of **k** points which are expected to be representative of the entire BZ. In the past, much effort has been devoted to developing an efficient set of **k** points that accurately describe the total energy and minimize the errors in the BZ sampling.[2–4] In particular, the uniform **k**-point mesh approach suggested by Monkhorst and Pack[4] (MP mesh) has been widely used in calculations of various solid state systems. For a given supercell, the total energy always converges as the density of the MP mesh is increased. Makov *et al.*[5] introduced an alternative scheme for sampling the BZ, in which the mesh depends on the lattice type. This sampling scheme has been shown to give faster convergence of the total energy using less **k** points for several systems.[6,7]

Among the many BZ sampling schemes developed for defect systems, the most popular approach is to use the Γ-point only with sufficiently large supercells. Γ-point sampling offers additional saving in computational resources because the wave functions are purely real. For small supercells, however, Γ-point sampling is insufficient to represent the whole BZ, and the total energy is quite different from that calculated using denser meshes. Nevertheless, Γ-point sampling has been used in many calculations based on the belief that systematic errors in total energies will tend to cancel out if the supercell sizes are the same. However, it has been reported that the errors do not cancel for some systems. For instance, the error caused by Γ-point sampling does not cancel for silicon vacancy[5] and interstitial[8] defects when taking the energy difference between defect-containing and perfect-crystal supercells. In addition, in Γ-point sampling of substitutional chalcogen defects in a silicon 54-atom supercell, the minimum in the plot of relative total energy versus the displacement of the chalcogen atom was erroneous.[9] The reconstruction energies of $p(2\times1)$ and $p(2\times2)$ Si(100) surfaces calculated using a supercell with 12-atom layers resulted in errors of more than 3 eV when Γ-point sampling was applied for the in-plane BZ, as shown by comparing the results to those obtained using the 2^3 MP mesh.[10] The formation energies of various self-interstitials in a silicon 16-atom supercell showed errors of about 1 eV for Γ-point sampling compared to 2^3 MP sampling.[11] Thus, the energy convergence of **k**-point meshes must be examined carefully, even with regard to the energy difference between very similar systems.

In addition to the total energy, atomic relaxation also depends on the BZ sampling density. It has been reported that atomic relaxation strongly depends on the **k**-point sampling, as relatively small errors in the total energy can lead to sub-

stantial errors in the atomic forces.[12] For example, Puska *et al.*[7] observed that the symmetry of the nearest neighbor atoms around a vacancy in silicon 32-, 64-, and 128-atom supercells depended on the **k**-point sampling. In addition, Clark and Ackland[13] found that, using a 64-atom silicon interstitial supercell, the calculated atomic forces at the Γ-point did not converge sufficiently to give a reliable defect structure. Further, in calculations using amorphous silicon supercells in the range of 32 to 54 atoms, Γ-point sampling led to significant errors in the atomic forces. These errors meant that an amorphous structure was obtained after simulated annealing by molecular dynamics, whereas equivalent calculations using 2^3 MP sampling gave a crystalline structure.[12]

In supercell calculations, consideration should be given not only to the convergence of the total energy with increasing BZ sampling density for a given supercell, but also to the supercell size dependence for well-converged **k**-point meshes. We have discussed the supercell size effect on the total energy of charged systems in an earlier paper.[14]

In the present study we investigate the **k**-point sampling effects on the formation energy and atomic relaxation of vacancies and interstitials in diamond and silicon for several supercell sizes up to 500 atoms and for various charge states.

II. COMPUTATIONAL METHODS

Our calculations were performed within density functional theory (DFT) using the fully self-consistent *ab initio* package SIESTA.[15] The spin polarized generalized-gradient approximation (sp-GGA), in particular the functional of Perdew, Burke, and Ernzerhof (PBE),[16] was used for the exchange-correlation energy. Only valence electrons were considered using numerical atomic orbitals, and their interactions with core electrons were modeled as norm-conserving scalar-relativistic pseudopotentials including nonlinear partial-core corrections. The real-space mesh grid was determined by the maximum kinetic energy of the plane waves (100 Ry). The electronic iterations were continued until the total energy differences between consecutive steps are smaller than 10^{-5} eV. The atomic geometries were relaxed until the largest atomic force was less than 10 meV/Å by means of a conjugate gradient scheme.

For the BZ integration, we used $n \times n \times n$ MP meshes that always included the Γ-point. We studied 2-, 8-, 16-, 32-, 64-, 128-, 216-, and 432-atom supercells, which have simple cubic (SC), face-centered cubic (FCC), or body-centered cubic (BCC) lattice symmetries depending on the supercell. First, the 2-atom perfect supercell was tested for convergence of the total energy with increasing n. We found that the total energy had fully converged for the $8 \times 8 \times 8$ MP **k**-point set. For larger supercells, we estimated the mesh parameter $p = 8(\Omega_2/\Omega_N)^{1/3}$ giving the same BZ sampling density as in the 8^3 **k**-point set of the 2-atom supercell ($\Omega_2/8^3$), where the BZ sampling density is defined as the reciprocal lattice volume per **k**-point (Ω_N/p^3). The optimal Monkhorst-Pack parameter n was defined as the nearest integer of p; hence the actual BZ sampling density, Ω_N/n^3, can show a small deviation. The BZ sampling densities of the 64- and 216-atom supercells were smaller than those of the other supercells.

TABLE I. Monkhorst-Pack test: The size of the supercell (N), the type of superlattice, the volume of the reciprocal lattice (Ω_N) relative to that of the 2-atom supercell, the **k**-point sets used for the calculations, and the corresponding BZ sampling density (BZSD).

N	Lattice	Ω_2/Ω_N	p	n	BZSD (Å^{-3})
2	FCC	1	8.00	8	0.042
8	SC	4	5.04	5	0.043
16	FCC	8	4.00	4	0.042
32	BCC	16	3.17	3	0.050
64	SC	32	2.52	3	0.025
128	FCC	64	2.00	2	0.042
216	SC	108	1.68	2	0.025
432	FCC	216	1.33	1	0.099

For the 432-atom supercell, Γ-point sampling does not seem to be sufficient from the viewpoint of BZ sampling density; however, it was used due to computational limitations. Table I lists the lattice symmetry, the reciprocal lattice volume of the N-atom supercell (Ω_N) relative to that of the 2-atom supercell (Ω_2), the values of p and n, and the corresponding BZ sampling densities. Recently, Probert and Payne[17] suggested that a BZ sampling density of $\leqslant 0.104$ Å^{-1} is required for the convergence of the vacancy formation energy with a tolerance of 0.01 eV for silicon. This sampling density was scaled to 0.021 Å^{-3} for our system.

The numerical atomic orbitals offer efficient basis sets because the number of basis functions needed is usually quite small.[15,18] However, they lack the systematics for testing the convergence of the basis set. The electronic configuration of atomic carbon in the ground state is s^2p^2; hence a single (S) zeta (Z) function for the s orbital and another for the p orbital is the minimal basis set (SZ). We investigated the effect of increasing the basis set to double (D) and triple (T) zeta basis sets, and of including single (P) and double polarization (DP) orbitals for the d orbitals.

To determine the optimal basis set, we calculated lattice constant, bulk modulus and its derivative, band gap, and cohesive energy of bulk diamond using a series of basis sets; the calculation results are summarized in Table II. Comparison of our results with those of previous well-converged plane-wave (PW) basis calculations and experiments indicates that the DZP basis set offers well-converged values. The seemingly good results for the band gap by SZ, DZ, and TZ are artifacts resulting from incorrect description of the conduction band eigenstates, which is improved by inclusion of the polarization orbital. The orbital ranges used for carbon are r_c=4.63 and 3.43 Bohr for s, r_c=5.66 and 3.65 Bohr for p, and r_c=5.66 Bohr for d. The orbital ranges for silicon are r_c=5.67 and 4.53 Bohr for s, r_c=7.11 and 5.20 Bohr for p, and r_c=7.11 Bohr for d. The calculated lattice constants are 3.59 and 5.51Å for diamond and silicon, respectively.

III. RESULTS AND DISCUSSION

A. Band structure

To estimate the required density of **k** points, we investigate the eigenvalue dispersion along **k**. The band structures

TABLE II. Basis comparisons for bulk diamond. The lattice constant, bulk modulus (B), and its derivative (B'), band gap (E_{gap}), and cohesive energy (E_c). B and B' are obtained using the Murnaghan equation of state. The number in parentheses of the first column is the number of basis functions.

Basis set	a (Å)	B (Mbar)	B'	E_{gap} (eV)	E_c (eV)
SZ(4)	3.62	3.84	3.65	5.76	6.86
SZP(9)	3.60	4.20	3.78	4.41	7.15
DZ(8)	3.60	4.01	3.99	5.58	7.35
DZP(13)	3.59	4.16	3.73	4.21	7.60
TZ(12)	3.60	3.91	3.95	4.99	7.40
TZDP(22)	3.58	4.33	3.64	4.18	7.66
PW(sp-GGA) (Ref. 19)	3.57	4.30	3.69	4.12	
PW(LDA) (Ref. 20)	3.62	4.38	3.5	4.03	7.9
Green's function (Ref. 21)	3.56	5.03	3.6		7.7
Expt. (Refs. 22 and 23)	3.567	4.43	4.0	5.49	7.37

of the *unrelaxed* neutral vacancy and interstitial defects in diamond for the 128-atom supercell, plotted in Fig. 1, indicate that the eigenvalues vary considerably in **k** space. For the vacancy, the lowest eigenvalue in the valence band and the t_2-defect levels change along Γ to X by 0.52 eV and 0.58 eV, respectively. The band structure of the interstitial shows the flat band corresponding to the s orbital of the interstitial atom at the bottom of the valence band. The dispersion energies of the second-lowest eigenvalue and t_2-defect level are 0.27 eV and 0.49 eV, respectively. The dispersion energy of the t_2-defect level decreases with increasing supercell size, as shown in Table III. Considering the dispersion of eigenvalues

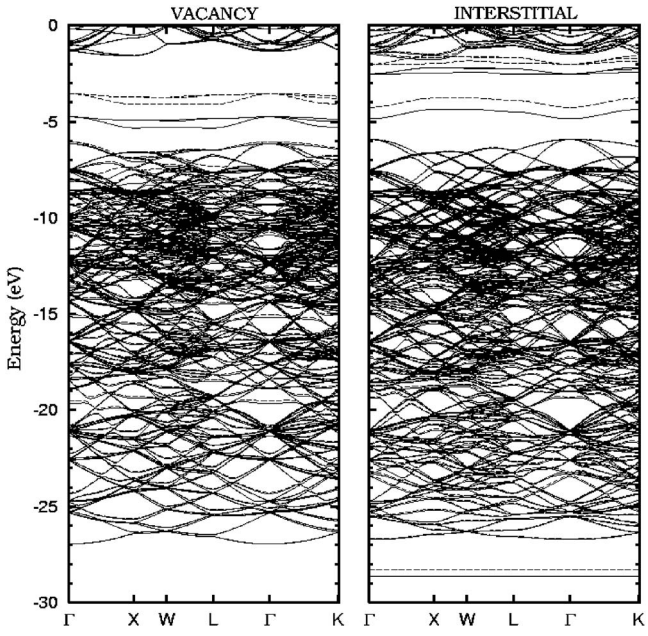

FIG. 1. The band structures of neutral vacancy and interstitial defects in diamond for a 128-atom supercell versus the high symmetry line in the BZ. The solid lines indicate the up-spin states and the dashed lines indicate down-spin states.

TABLE III. Band dispersion energies of the t_2-defect levels of neutral vacancy and interstitial defects in diamond. The energy unit is eV.

Supercell size	32	64	128	216
Vacancy	1.1764	0.8439	0.5865	0.1804
Interstitial	0.9059	0.5697	0.5069	0.1162

along **k**, more than one **k** point would be required to accurately calculate the total energy and wave functions.

The total valence band widths are 20.82 eV and 20.81 eV (22.74 eV including the lowest band resulting from the interstitial s orbital) for the vacancy and interstitial, respectively. For bulk diamond, the calculated band width is 21.1 eV. (The experimental band width is 23 ± 0.2 eV.[24,25]) Thus the bandwidths of the defect-containing supercells are smaller than that of the bulk supercell.

B. Dependence of formation energy on *k*-point sampling

To investigate the **k**-point sampling effect on the total energy, we calculate the total energy difference per atom between the Γ-point and 2^3 MP sampling methods:

$$\Delta E^q_{tot}/N = [E^q_{tot}(\Gamma) - E^q_{tot}(2^3)]/N, \quad (1)$$

where E^q_{tot} is the total energy of an N-atom supercell with a charge state q. The results of the calculations for vacancies and interstitials in diamond are plotted in Fig. 2 for the possible charge states of $+2$, $+1$, 0, -1, -2, -3, and -4. For all

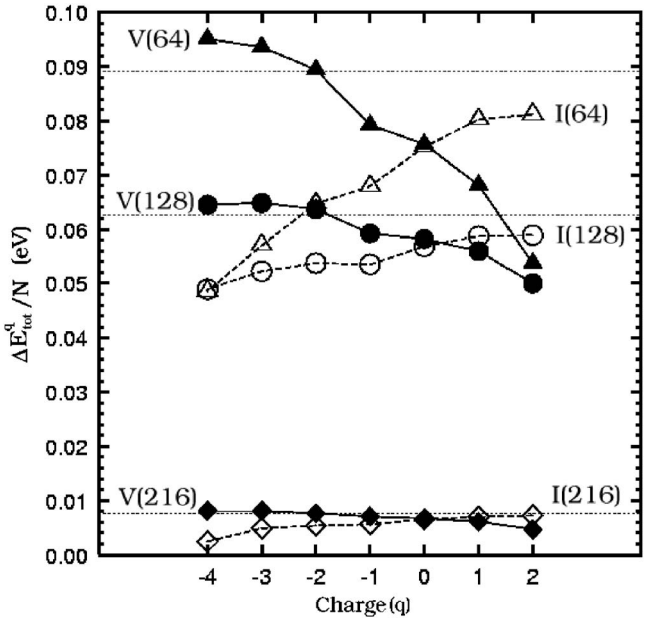

FIG. 2. The total energy difference per atom between Γ-point and 2^3 MP **k**-point sampling for 64 (triangle)-, 128 (circle)-, and 216 (diamond)-atom supercells. Vacancies and interstitials are represented by filled and empty symbols, respectively. The $\Delta E^q_{tot}/N$ values of the bulk 64-, 128- and 216-atom supercells are drawn as dotted horizontal lines from top to bottom.

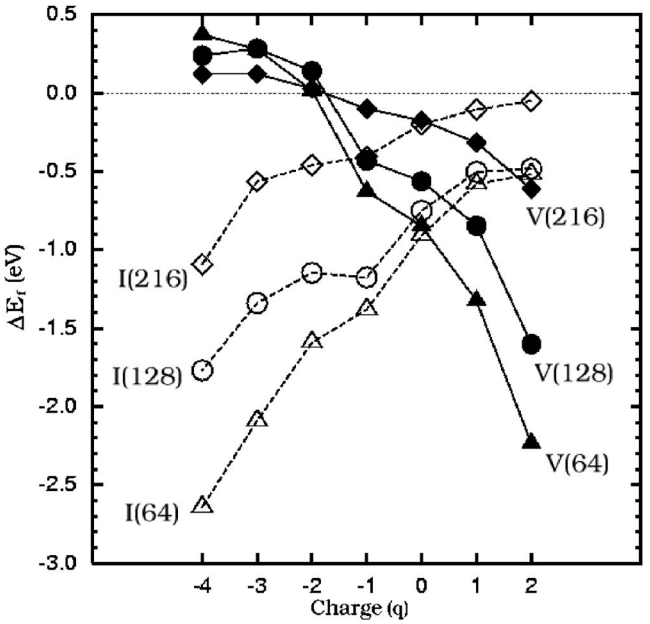

FIG. 3. The **k**-point sampling error in the formation energy for the 64 (triangle)-, 128 (circle)-, and 216 (diamond)-atom supercells. Both vacancy and interstitial data are presented (filled and empty symbols, respectively).

of the charge states, the total energies calculated by Γ-point sampling are higher than those calculated by 2^3 MP sampling. $\Delta E^q_{tot}/N$ increases with decreasing supercell size for all charge states of both defect types, which is consistent with the fact that the dispersion of eigenvalues is larger for smaller supercells. It is notable that the **k**-point sampling error varies considerably depending on the type and charge state of the defect, even for systems with the same supercell size. For the 128-atom supercell, for instance, $\Delta E^q_{tot}/N$ is 0.050, 0.065, 0.059, and 0.049 eV for V^{+2}, V^{-4}, I^{+2}, and I^{-4}. The total energy difference decreases as the vacancy becomes more positively charged and the interstitial becomes more negatively charged, i.e., the difference is inversely proportional to the electronic perturbation of the defect system relative to the perfect bulk system.

This difference in the total energy should also be reflected in the formation energy. Since the formation energy is related to the total energy of the bulk supercell, it is important to investigate the **k**-point sampling error of the defect system relative to that of the perfect bulk system. As seen in Fig. 2, the **k**-point sampling error in the total energy of the perfect bulk system is closest to that of the defect system with the least perturbation. Therefore, the **k**-point sampling error in the formation energy would be expected to increase as the electronic configuration of the defect system is increasingly perturbed from that of the bulk.

To investigate the Γ-point sampling error in the formation energy, the values of the formation energy difference, $\Delta E^q_f(N)$, are calculated for various supercells with charge state q (Fig. 3), where

$$\Delta E^q_f(N) = E^q_f(N,\Gamma) - E^q_f(N,2^3). \tag{2}$$

The formation energy E^q_f is given by

TABLE IV. Ionization levels of the *unrelaxed* vacancies and interstitials in diamond supercells. The ionization levels between thermodynamically stable states within the calculated band gap are shown in boldface. All values are in eV.

	(+2/+)	(+2/0)	(+/0)	(0/−)	(−/2−)	(0/2−)
V(128)-Γ	**0.897**	0.981	**1.065**	**1.389**	**3.444**	2.416
V(128)-2^3	**0.168**	0.478	**0.787**	**1.256**	**2.871**	2.064
V(216)-Γ	**0.725**	0.799	**0.873**	**1.248**	**3.358**	2.303
V(216)-2^3	**0.436**	0.580	**0.725**	**1.170**	**3.229**	2.200
I(128)-Γ	**2.596**	2.828	**3.061**	**3.424**	**4.133**	3.778
I(128)-2^3	**2.617**	2.963	**3.309**	**3.848**	**4.106**	3.977
I(216)-Γ	**2.578**	2.850	**3.121**	**3.543**	**4.102**	3.822
I(216)-2^3	**2.625**	2.922	**3.219**	**3.750**	**4.156**	3.953

$$E^q_f = E^q_{tot} - N\mu + q(E_V + \mu_e), \tag{3}$$

where E^q_{tot} is the total energy of the defect-containing system made up of N atomic species, with atomic chemical potential μ. We use the valence band maximum of bulk supercell as E_V for all the systems.

As expected, the **k**-point sampling error in the total energy is reflected in a considerable error in the formation energy, as shown in Fig. 3. As in the error in the total energy, the error in the formation energy also depends on the defect type and charge state. For the 128-atom vacancy supercell, the error in the formation energy is about 1.6 eV for V^{+2} and then decreases as the charge state becomes more negative. On the other hand, the error for the interstitial system is largest for I^{-4} by about 1.8 eV and decreases as the charge state becomes more positive. The ionization levels, given in Table IV, also change considerably depending on the **k**-point set. Since the **k**-point sampling error in the formation energy varies depending on the charge state, it should remain in the ionization levels without systematic cancellation even for the same size of supercell. In the 216-atom supercell, for example, the ionization level errors of V^{+2}/V^{+1} and I^0/I^{-1} are about 0.3 eV and 0.2 eV, respectively.

To understand the origin of the Γ-point sampling error dependence on the charge state and the defect type, we investigate the electronic structure in detail by examining the standard deviation of the density of states $D(E)$,

$$\sigma^2 = \langle D(E)^2 \rangle - \langle D(E) \rangle^2. \tag{4}$$

If each eigenvalue varies more (less) in **k** space, then σ^2 will be smaller (larger) and the total energy will converge more slowly (quickly) with increasing BZ sampling density, which will result in a larger (smaller) Γ-point sampling error. Figure 4 shows a strong correlation between the Γ-point sampling error in the total energy and σ^2; the order of σ^2 is the opposite of that of $\Delta E^q_{tot}/N$. When the symmetry of the perfect crystal is reduced by defects, impurities, or lattice distortions, the extent of electronic delocalization will be reduced, and the resulting localization of electronic states should lead to an increase in σ^2. Indeed, as seen in Fig. 4, σ^2 increases with increasing deviation of the electronic configu-

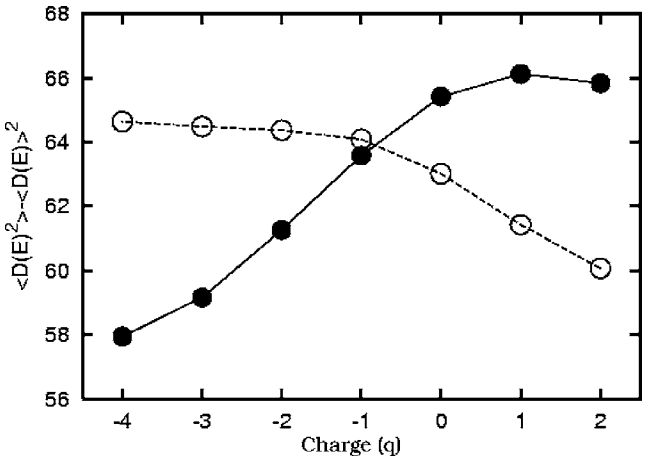

FIG. 4. The standard deviation of $D(E)$, σ^2, of vacancy (filled circles) and interstitial (empty circles) defects in diamond for a 128-atom supercell. $D(E)$ is calculated by numerical integration over 30000 energy points for filled energy levels with a Gaussian smear of 0.2 eV.

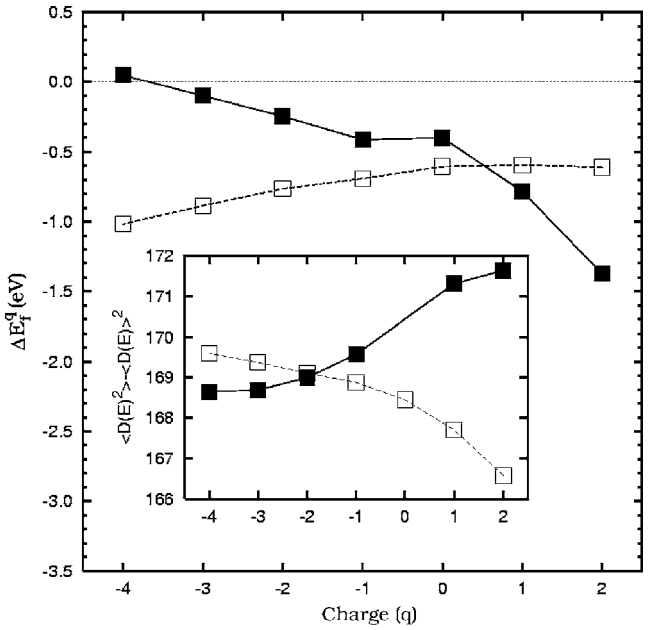

FIG. 5. The **k**-point sampling error in the formation energy of the 128-atom supercell for *silicon* vacancy and interstitial defects (filled and empty symbols respectively). Inset shows the standard deviations of $D(E)$ of the corresponding systems.

ration from the bulk configuration (more positive charge state for vacancies and more negative charge state for interstitials). To confirm this trend, we performed calculations for a diamond structure containing a divacancy using a 64-atom supercell, a system whose symmetry is lower than that of the monovacancy system, and found that the total energy difference between the Γ-point and 2^3 MP samplings was smaller than that of the monovacancy system.

In addition to diamond supercells, we also studied silicon supercells. Similar to the case of diamond, the **k**-point sampling error in the total energy of the silicon system decreases with increasing perturbation of the electron density. These noncancelling **k**-point sampling errors are transferred into the formation energy, as can be seen in the 128-atom-supercell data presented in Fig. 5. $E_f^q(\Gamma)$ is smaller than $E_f^q(2^3)$ for all the charge states (data not shown). The noncancelling **k**-point sampling error of ΔE_f^q can be explained by the standard deviation of $D(E)$, as shown in the inset in Fig. 5. In addition, the ionization levels are listed in Table V. The Γ-point method gives particularly large errors for the values related to the positive charge states of vacancies. It erroneously stabilizes V^{+2} and V^{+1} which could not be thermodynamically stable in the range of the band-gap for 2^3 MP sampling.

C. Dependence of atomic relaxation on *k*-point sampling

For vacancies in diamond, we investigate the defect-induced atomic relaxations for various charge states. For all the supercells considered, the outward relaxations of the four atoms around the vacancy (first-shell atoms) conserve the T_d symmetry. The change of volume $(\Delta V(N,k)=(V(N,k)-V_0)/V_0\times 100\%)$ of the tetrahedral structure defined by the first-shell atoms is calculated using the Γ-point and 2^3 MP samplings. For the 216-atom supercell sampled using the 2^3 MP mesh, the tetrahedron volume is expanded relative to the initial unrelaxed volume by 73.5%, 61.1%, 50.7%, and 43.4% for the +2, +1, 0, and −1 charge states, respectively.

The difference between $\Delta V(N,\Gamma)$ and $\Delta V(N,2^3)$ as a function of charge is plotted in Fig. 6 for several supercells. In most cases the relaxed tetrahedron volume is larger for Γ-point sampling and becomes much larger as the charge state becomes more negative. The large volume relaxation in the Γ-point sampling can be explained by the electron configuration in the defect level. Triply degenerate eigenstates of the t_2-defect level at Γ-point split into three levels with different energies at other **k** points. The dispersion energy of the split eigenvalue is over 0.5 eV along Γ to X for the 128-atom supercell, as shown in Fig. 1. The triply degenerate wavefunctions at the Γ-point overlap in space, whereas the split wavefunctions at other **k** points are separated. Therefore, the defect-related electrons at the Γ-point will feel a stronger repulsion than those at other **k** points, and hence will have a greater tendency to move away from each other. Consequently, the tetrahedron volume calculated by Γ-point sam-

TABLE V. Ionization levels for the *unrelaxed* vacancies and interstitials in silicon supercells. The ionization levels between thermodynamically stable states within the calculated band gap are shown in boldface. Dashes indicate cases where the calculations gave negative ionization levels, which are unphysical. All values are in eV.

	(+2/+)	(+2/0)	(+/0)	(0/−)	(−/2−)	(0/2−)
V(128)-Γ	**0.418**	0.435	**0.453**	**0.531**	0.834	0.682
V(128)-2^3	—	—	**0.068**	**0.546**	0.666	0.606
I(128)-Γ	**0.566**	0.574	**0.582**	0.617	0.691	0.654
I(128)-2^3	**0.550**	0.572	**0.593**	0.703	0.763	0.733

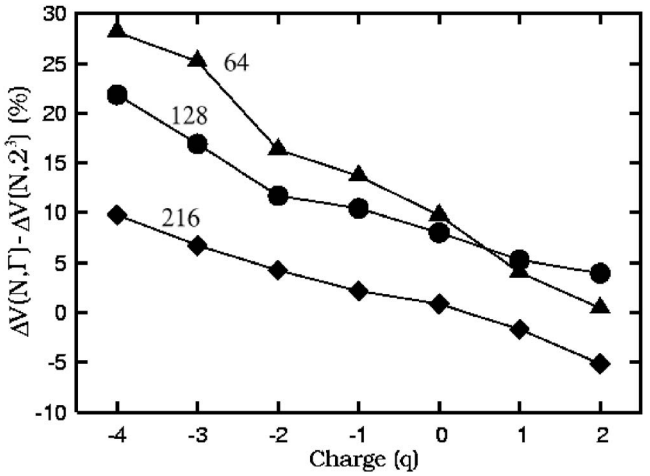

FIG. 6. Difference between $\Delta V(N,\Gamma)$ and $\Delta V(N,2^3)$ of the four atoms nearest to the vacancy between 2^3 MP and Γ**k**-point sampling for 64 (triangle)-, 128 (circle)-, and 216 (diamond)-atom supercells.

pling is larger than that calculated by 2^3 MP sampling. This repulsive force becomes stronger as the electron density in the defect level increases; hence the tetrahedron volume difference between the Γ-point and 2^3 MP samplings increases as the charge state becomes more negative.

The importance of BZ sampling density has also been emphasized in respect to the finite-temperature properties of amorphous materials. Drabold *et al.*[12] found that the Γ-point method leads to a spurious minimum in the configurational potential energy of the amorphous silicon system, and concluded that the unphysically small restoring force on the silicon atoms (i.e., the force that favors their return to their initial diamond structure positions) results in an erroneously strong diffusion.

IV. CONCLUSIONS

The dependence of the formation energy and atomic structure on the BZ sampling density have been investigated for vacancy and interstitial defects using DFT. It has been generally believed that the systematic error induced by use of too small **k**-point set would cancel out for systems of similar or identical size. However, we find that the systematic errors in the total energy and atomic relaxation of a defect do not cancel, and that they vary considerably depending on the charge state and defect type, even for the same size of supercell. The non-cancelling **k**-point sampling error in the total energy is transferred to the formation energy, and consequently seriously affects the prediction of thermodynamically stable states and ionization levels. The **k**-point sampling error in the total energy increases as the number of electrons in the system approaches that in the bulk, while the error in the formation energy decreases.

We analyze quantitatively the origin of the **k**-point sampling error by examining the standard deviation of $D(E)$. Based on these results, we conclude that the symmetry reduction associated with the presence of a defect induces the localization of electronic states, causing the **k**-point sampling error to become smaller for more disordered structures.

The BZ sampling density affects not only the energetics but also the atomic forces, which in turn affect the atomic structure and molecular dynamics trajectories. We investigate the vacancy system of diamond, in which atoms neighboring the vacancy undergo considerable outward relaxation. The Γ-point method gives erroneously large atomic relaxations due to the strong repulsion between electrons in degenerate defect levels, and this error increases in proportion to the number of electrons in the defect level.

ACKNOWLEDGMENTS

This work was supported by the Korean Research Foundation through the research contract of 2002-070-C00048, and the Academy of Finland through the Center of Excellence Program (2002-2005). We acknowledge the generous provision of computing resources by the Center for Scientific Computing (CSC), Espoo, in Finland.

[1] N. W. Ashcroft and N. D. Mermin, *Solid State Physics* (1976).
[2] A. Baldereschi, Phys. Rev. B **7**, 5212 (1973).
[3] D. J. Chadi and M. L. Cohen, Phys. Rev. B **8**, 5747 (1973).
[4] H. J. Monkhorst and J. D. Pack, Phys. Rev. B **13**, 5188 (1976).
[5] G. Makov, R. Shah, and M. C. Payne, Phys. Rev. B **53**, 15513 (1996).
[6] D. J. Chadi, P. H. Citrin, C. H. Park, D. L. Adler, M. A. Marcus, and H.-J. Gossmann, Phys. Rev. Lett. **79**, 4834 (1997).
[7] M. J. Puska, S. Pöykkö, M. Pesola, and R. M. Nieminen, Phys. Rev. B **58**, 1318 (1998).
[8] J. Lento, J.-L. Mozos, and R. M. Nieminen, J. Phys.: Condens. Matter **14**, 2637 (2002).
[9] J. Furthmüller and M. Fähnle, Phys. Rev. B **46**, 3839 (1992).
[10] A. Ramstad, G. Brocks, and P. J. Kelly, Phys. Rev. B **51**, 14504 (1995).
[11] R. J. Needs, J. Phys.: Condens. Matter **11**, 10437 (1999).
[12] D. A. Drabold, J. D. Dow, P. A. Fedders, A. E. Carlsson, and O. F. Sankey, Phys. Rev. B **42**, 5345 (1990).
[13] S. J. Clark and G. J. Ackland, Phys. Rev. B **56**, 47 (1997).
[14] J. Shim, E.-K. Lee, Y.-J. Lee, and R. M. Nieminen, Phys. Rev. B **71**, 035206 (2005).
[15] J. M. Soler, E. Artacho, J. D. Gale, A. García, J. Junquera, P. Ordejón, and D. Sánchez-Portal, J. Phys.: Condens. Matter **14**, 2745 (2002); D. Sánchez-Portal, P. Ordejón, E. Artacho and J. M. Soler, Int. J. Quantum Chem. **65**, 453 (1997); P. Ordejón, E. Artacho and J. M. Soler, Phys. Rev. B **53**, R10441, (1996).
[16] J. P. Perdew, K. Burke, and M. Ernzerhof, Phys. Rev. Lett. **77**, 3865 (1996).
[17] M. I. J. Probert and M. C. Payne, Phys. Rev. B **67**, 075204 (2003).
[18] E. Anglada, J. M. Soler, J. Junquera, and E. Artacho, Phys. Rev. B **66**, 205101 (2002); E. Artacho, D. Sánchez-Portal, P. Orde-

jón, A. García, and J. M. Soler, Phys. Status Solidi B **215**, 809 (1999); J. Junquera, Ó. Paz, D. Sánchez-Portal, and E. Artacho, Phys. Rev. B **64**, 235111 (2001).
[19] P. Lehtinen, Y. J. Lee, and R. M. Nieminen (unpublished).
[20] J. Bernholc, A. Antonelli, T. M. Del Sole, Y. Bar-Yam, and S. T. Pantelides, Phys. Rev. Lett. **61**, 2689 (1988).
[21] G. B. Bachelet, G. A. Baraff, and M. Schlüter, Phys. Rev. B **24**, 4736 (1981).
[22] M. T. Yin, Phys. Rev. B **30**, 1773 (1984).
[23] M. T. Yin and M. L. Cohen, Phys. Rev. B **24**, 6121 (1981).
[24] I. Jiménez, L. J. Terminello, D. G. J. Sutherland, J. A. Carlisle, E. L. Shirley, and F. J. Himpsel, Phys. Rev. B **56**, 7215 (1997).
[25] P. W. Anderson, Phys. Rev. **109**, 1492 (1958).